IEEE Access
Multidisciplinary | Rapid Review | Open Access Journal

Received 17 September 2022, accepted 30 September 2022, date of publication 10 October 2022,
date of current version 31 October 2022.

Digital Object Identifier 10.1109/ACCESS.2022.3213725

RESEARCH ARTICLE

ESPotensio: A Low-Cost and Portable Potentiostat With Multi-Channel and Multi-Analysis Electrochemical Measurements

ISA ANSHORI[1,2], IQBAL FAWWAZ RAMADHAN[1], EDUARDUS ARIASENA[1], RIKSON SIBURIAN[3,4], JON AFFI[5], MURNI HANDAYANI[6], HENKE YUNKINS[7], TOMOAKI KUJI[8], TATI LATIFAH ERAWATI RAJAB MENGKO[1], AND SUKSMANDHIRA HARIMURTI[1]

[1]Lab-On-Chip Group, Department of Biomedical Engineering, School of Electrical Engineering and Informatics, Institut Teknologi Bandung, Bandung 40132, Indonesia
[2]Research Center for Nanoscience and Nanotechnology, Institut Teknologi Bandung, Bandung 40132, Indonesia
[3]Department of Chemistry, Faculty of Mathematics and Natural Sciences, Universitas Sumatera Utara, Medan 20155, Indonesia
[4]Carbon Research Center, Universitas Sumatera Utara, Medan 20155, Indonesia
[5]Mechanical Engineering Department, Engineering Faculty, Universitas Andalas, Padang 25163, Indonesia
[6]Research Centre for Advanced Materials—National Research and Innovation Agency (BRIN), Tangerang Selatan 15314, Indonesia
[7]Trillium Technologies Indonesia, Jakarta 40184, Indonesia
[8]Research and Development Division, Blue Industries Inc., Sumida, Tokyo 130-0013, Japan

Corresponding authors: Isa Anshori (isaa@staff.stei.itb.ac.id) and Suksmandhira Harimurti (sukman@staff.itb.ac.id)

This work was supported in part by the Bandung Institute of Technology through Riset Kolaborasi Indonesia (RKI) 2022 with grant number of LPPM.PN-6-83-2022; and in part by the Ministry of Education, Culture, Research, and Technology of The Republic of Indonesia for the Grant Scheme of Penelitian Dasar Unggulan Perguruan Tinggi (PDUPT) under Grant number 2/AMD/E1/KP.PTNBH/2020. We also acknowledge analytical instrumentation facility from ELSA (E-Layanan Sains) – National Research and Innovation Agency (BRIN).

ABSTRACT Electrochemical measurement methods are widely used to analyze various biochemical reactions due to their simplicity and versatility. Therefore, the development of potentiostats, electrochemical-based analytical instruments, that are low in cost but maintaining rich analytical features is highly demanding. In this paper, we report the development of a low-cost and portable potentiostat system, named ESPotensio, which supports six different electrochemical measurement methods and a multi-channel electrochemical measurement. The measurement methods it supports include the cyclic voltammetry (CV), linear sweep voltammetry (LSV), square wave voltammetry (SWV), differential pulse voltammetry (DPV), normal pulse voltammetry (NPV), and the observation of electrochemical response current against time based on chronoamperometry (CA) measurement method. Moreover, each of these measurement methods can be run semi-parallelly within three different channels. The electrochemical measurement precision, accuracy, and error of ESPotensio were evaluated based on the repeated measurements and the comparison with the commercial potentiostats. The results showed that it could produce highly accurate electrochemical measurements by having an average accuracy of more than 90% compared to the commercial potentiostat, Emstat Pico. Ultimately, the hardware design was determined accordingly to meet the low-cost demand by costing of only USD 21.4 for the total system realization.

INDEX TERMS Potentiostat, electrochemical, multi-channel, voltammetry, chronoamperometry, microcontroller.

I. INTRODUCTION

The biosensor technology development faces a big challenge as a point-of-care (POC) testing, especially in realizing an affordable system while maintaining its measurement sensitivity and selectivity. In addition, the trend of POC also requires high portability, user-friendliness, integration easiness, automatic operation, and multiplexing measurement [1]. Therefore, there is a current trend of manufac-

The associate editor coordinating the review of this manuscript and approving it for publication was Lei Wang.

turing portable potentiostats. Recently, many manufacturers launched portable potentiostats which can perform various electrochemical measurements comparable to the conventional system, such as Metrohm Autolab's mini PSTAT and the Palmsens' Emstat. However, these potentiostats are still expensive, about several thousand dollars. Besides, there is another limitation related to the few sources of information about these products due to proprietary reasons on components and circuit designs.

On the other hand, a low-cost potentiostat will not only benefit public health facilities or clinics but also educational institutions by providing tools for simple biochemical analysis introductions [2]. Hence, the development of a low-cost portable potentiostat has been flourishing ever since. Several studies have developed potentiostat that can be operated using Android applications on mobile phones, and using computer or laptop via Labview, Matlab, R environment, Python, and Microsoft Excel. Huang et al. conducted a study of integrating a homemade potentiostat using Labview [3]. Sarkar et al. integrated the potentiostat via Bluetooth and WiFi, while the GUI was developed based on Matlab [4]. Moreover, Ministat, according to a study by Adams et al., uses the R environment for the graphical user interface (GUI) [5], while Pansodtee uses Python [6]. In contrast, Bukkawar et al. used just Microsoft Excel as the GUI [7]. In addition, several electrochemical instruments to support the education in chemistry have also been developed. The implementation was carried out by manufacturing electrochemical instruments using microcontroller-based potentiostats. Several studies that implement microcontroller-based potentiostats, including those conducted by Melenbrink et al. who used Arduino [8], Glasscott et al. used Teensy [9], Adams et al. used ATxmega32E5 [7], and Ning et al. used STM32 [10].

Furthermore, a more flexible potentiostat by providing multichannel features to simultaneously perform measurements with many channels has also been developed [6]. However, this potentiostat was developed by making the potentiostat modular in its channel measurement, making the cost to fabricate the potentiostat relatively more expensive, with an average cost of around USD 100 per module. Thus, there is still a great demand for developing potentiostats with a good measurement performance, easy operation, support multiple measurement modes, multi-channel capabilities, and support a portability use by using a mobile phone or laptop connection.

On the other hand, low-cost potentiostats also need to support to several measurement methods based on their implementations. Cyclic Voltammetry (CV) is the typical or basic analysis tool to analyze various redox reactions, which include drug quality evaluation in pharmaceuticals, determination of phenolics and antioxidants in foods, and detection of biomolecules such as hormones. CV studies were used to detect several diseases in the medical field, such as abetalipoproteinemia, cancer, cerebral ischemia, and diabetes [11]. Another study used linear sweep voltammetry (LSV) to determine the levels of vortioxetine hydrobromide (VOR), which is an antidepressant drug with a high binding affinity to various serotonin receptors in the central nervous system [12]. Differential pulse voltammetry (DPV) assisted the process of determining and quantifying several contaminant substances of water sources by anthropogenic activity [13]. Square wave voltammetry (SWV) helped to understand the mechanism of action of drugs, the acid-base dissociation constant or pKa [14]. In other fields besides the medical, normal pulse voltammetry (NPV) have been used to detect leuco-indigo, which plays a role in dyeing clothes Aizome, Japanese indigo-dyeing [15]. These measurement methods can be integrated as a complementary in supporting the results from other measurement methods, such as chronoamperometric (CA), which is a complementary part of the CV measurements used for the measurement of glyphosate (GLY), a broad-spectrum herbicide and pesticide whose function is to assess the ecotoxicological impact [16]. Thus, our work aims to implement several electrochemical methods to increase the practical value of potentiostats in much wider applications. Another main feature that ESPotensio has is the ability to perform simultaneous measurements. Semi-parallel measurement feature is intended to increase the effectiveness of use, where users can easily analysis three different samples for one measurement method and the same measurement parameters to speed up the data collection process by eliminating the repetitive processes. In summary, the comparison of the reported low-cost microcontroller-based potentiostats (including our ESPotensio) is shown in Table 2. It can be clearly seen that ESPotensio has the lowest production costs (USD ∼21). Besides, ESPotensio also has an advantage in the GUI application, which can be operated wirelessly using Android application or via a wired PC connection by a Python-based application. Furthermore, ESPotensio can support up to 6 different measurement methods, which is the most among other low-cost microcontroller-based potentiostats.

This paper is divided into four sections: introduction, materials and methods, results and discussion, and conclusions. In the introduction section, the background of the research on low-cost and portable potentiostat along with the previous studies is thoroughly described. The second section discusses the materials and equipment required to assemble the ESPotensio, where we describe in detail the potentiostat subsystems, including the hardware architecture, signal acquisition, and communications subsystems. The third section contains the results and discussion, where we provide comprehensive technical comparison aspects of our proposed system with the other low-cost potentiostats. The final section contains a summary or conclusion to this paper. For convenience, the summary of abbreviations is also provided in Table 1.

II. MATERIALS AND METHODS

A. MATERIALS, INSTRUMENTS, AND SOFTWARE

The Ltspice XVII(x64) software (LTspice®Linear Technology Corporation, US Pacific) was used to conduct the circuit simulation and to verify the potentiostat analog circuit design

TABLE 1. Summary of abbreviations.

ADC	analog-to-digital converter
AMPA	aminomethylphosphonic acid
ASV	anodic stripping voltammetry
BLE	Bluetooth Low Energy
CA	chronoamperometric
CC	chronocoulometry
CE	counter electrode
CV	cyclic voltammetry
DAC	digital-to-analog converter
DPV	differential pulse voltammetry
GUI	graphical user interface
LPF	low-pass filter
LSV	linear sweep voltammetry
NPV	normal pulse voltammetry
PBS	Phosphate Buffer Saline
POC	point-of-care
RE	reference electrode
SPE	screen-printed electrode
SWV	square wave voltammetry
WE	working electrode

before printing the PCB. PCB design boards and analog components were purchased from local stores. The assembled analog circuit was integrated with the ESP32 microcontroller (Espressif Systems, Shanghai, China). For the voltage source, there were two options, when using Bluetooth communication, the tag source was supplied by 4 AA 1.5V batteries arranged in series, while for cable communication, the power was supplied via USB. For positive voltage, it used a 3.3V voltage from the ESP32, which was then increased to 5V using the MT3608 module (Aerosemi technology Co. ltd, Shaanxi, China). For the negative voltage source, the LM2662 module (Lisu Instrument, Depok, Indonesia) was used. This study also uses the MCP4725 module (Microchip Technology Inc., Chandler, Arizona) as the DAC. Arduino IDE 1.8.9 software (Arduino®, Arduino LLC, Boston, USA) was used to program the ESP32 microcontroller. This study also builds an Android application designed using the Android Studio platform (Google, California, USA) to test the ESP32 Bluetooth communication sub-system and an application for desktops using Python (Python Software Foundation, Delaware, USA). The electrochemical measurement performance of the constructed ESPotensio potentiostat instrumentation system was evaluated using potassium hexacyanoferrate(III) ($K_3[Fe(CN)_6]\cdot 3H2O$) purchased from Sigma Aldrich, Missouri, USA. This electrolyte solution was prepared in Phosphate Buffer Saline (PBS) (pH 7.4) solution purchased from Biogear. The SPE used in the electrochemical test were purchased from Zimmer&Peacock (Royston, UK) and Metrohm DropSens (Oviedo, Spain). In addition, to compare our potentiostat, Emstat Pico (PalmSens BV, Houten, Netherlands) was used, which we customized using the USB to TTL CP2102 module (Silicon Labs, Austin, USA).

B. GENERAL SYSTEM

The overall system is illustrated in Fig. 1a, which was divided into several large parts. The first relates to the application, a GUI that will be the liaison between the user and the potentiostat. Some of the main features in the application are the settings for determining the connection to the potentiostat, adjusting measurement parameters, and displaying measurement results and analysis. In this study, there are two kinds of applications made to be GUI: i.e. the Android smartphone app and the Python application for desktops (PCs/laptops). Both applications have the same main function with the addition of several features that are suitable for their respective platforms. The next part is the potentiostat. The potentiostat is connected to the disposable sensor based on a screen-printed electrode (SPE), which has a three-electrode configuration: working electrode (WE), reference electrode (RE), and counter electrode (CE). The SPE is the platform to read the response signal from the analyte, which is dropped on the sensing area of the SPE. The WE will read the electrochemical characteristics of the analyte. In general, the characteristics to be observed are the current and potential differences. The reading results from the potentiostat will then be sent to the GUI and reprocessed to show the measurement results as a graphic or file in CSV format.

Fig. 1b describes how users run the application to operate ESPotensio. First, the user enters the application. The selection of this application is determined by what communication method will be used: if using Bluetooth, the user needs to open the Android application, and if using a computer, the user opens a python-based application that has been provided. The user then chooses what measurement method and how many channels will be used. Determining the number of channels will affect the SPE, analyte, and connector to be used. After the user has properly configured the need, the user sets up the instrument and enters the desired measurement parameters. The potentiostat runs the measurement and will display the results at the end of the measurement. If the results do not match, the user needs to press the reset button on the application and potentiate it to re-enter the desired parameters. If the results are appropriate, the user will save the measurement results and continue for further analysis.

C. HARDWARE ARCHITECTURE

Fig. 2 shows the schematic design of the analog circuit of our proposed potentiostat. Vin is the input of the analog circuit that will be the task of the DAC module. The consideration of using the DAC module is that the DAC of ESP32 has an 8-bit resolution in the 0–3.3V range. The smallest resolution given to this circuit is at 0.0128 V or 12.8 mV. Using an external DAC module, a higher resolution is obtained at 12 bits with the smallest resolution value of 0.0008 V or 0.8 mV.

The first block of the circuit is a buffer circuit that has a large input resistance but a small output resistance so that the output voltage is the same as the input voltage. By using this configuration, the buffer circuit can supply a large amount of electrical energy by requiring small energy at the input pins. This also means that the DAC signal can be ensured not to be weakened. Using a summing amplifier, the DAC value of the microcontroller will be converted into a sweep

TABLE 2. Main features comparison of reported low-cost microcontroller-based potentiostats.

Ref.	Price (USD)	Communication Interfaces	Microcontroller	Experimental Capabilities	Number of Channel
[3]	Unreported	USB	C8051F005	CV	1
[4]	50	Bluetooth, Wifi	ESP 32, Arduino Uno	CV, LSV, CA	1
[5]	Unreported	USB	ATxmega32E5	CV, LSV, SWV, ASV, CA	1
[7]	Unreported	USB	ATmega328	LSV	1
[8]	40	USB	Arduino Uno	CV, LSV, CA	1
[9]	55	USB	Arduino Teensy 3.2	CV, LSV, CA, CC	1
[10]	Unreported	USB	STM32F103RCT6	Unreported	1
[17]	226.22	USB	PIC16F1459	CV	1
[18]	Unreported	NFC	CHI 611E	CV, CA	1
[19]	23–25	Bluetooth	Arduino Nano	CV, LSV, CA	1
[20]	Unreported	Bluetooth	LMP91000	CV, CA	1
[6]	~180	Wifi,USB	Raspberry Pi 3 B+	CV	Modular (up to 64)
[21]	Unreported	USB	LMP91000, ARM Cortex-M0 and SAMD21	CV, SWV, NPV, CA	1
[22]	~100	USB	ATmega328	LSV, CV, SWV	1
[23]	Unreported	Wifi	Custom-designed AFE and CC3200 Wifi	DPV, CA, SWV	1
[24]	Unreported	Wifi	ARM Cortex-M4 and CC3200	DPV	1
[25]	25.12	Bluetooth	ESP 32	CV	1
This work	21.4	Bluetooth, USB	ESP 32	CV, LSV, DPV, SWV, NPV, CA	3

voltage by combining it with a voltage of −5 V. Vo will be −1.5 V for Vpwm 3.3 V and 1.5 V for Vpwm 0 V. The voltage resolution value generated from the summing amplifier block is 3 V/4096 = 0.0007 V or 0.7 mV. In addition, to smoothen the signal output, a passive capacitor configured as a low-pass filter (LPF) with a cut-off frequency of 53.05 Hz was added to the circuit. However, it should be noted that adding a filter component presents a trade-off, where the signal will take time to reach a steady state.

The next blocks are three electrochemical cells containing three electrodes connection: WE, RE, and CE. In our study, we prepared 3 ports that can be connected to the SPE electrodes so that it is possible to take measurements simultaneously for 3 electrodes at once. Following this section, the other sections use the same circuit up to the ADC microcontroller. The addition of the port for this electrode cell can be varied to a certain amount while paying attention to the current and voltage supply that enters the electrode and allowing electrochemical reactions to occur. We also need to consider the energy supply from energy sources to see the duration of battery life if using batteries. The principle of this circuit is the same as that of a buffer circuit, in which the non-inverting input pin receives a sweep voltage signal from the summing amplifier block. On the other hand, the inverting input pin is connected to RE, while the output pin is connected to CE. The feedback from this block comes from the CE and RE, and the WE will be the sensing electrode, which carries the current measurement from the electrochemical cell block.

The following circuit block was implemented using a transimpedance amplifier and because we implemented a multichannel capability, so that the pair of resistors in this circuit consists of 3 pairs: R4 with R5, R7 with R8, and R10 with R11. By using R4, R7, R10 = 3.3 kΩ, and R5, R8, R11 = 10 kΩ, the value to be achieved is in the range of −500 μA to 500 μA. So, with the calculation, the current-to-voltage conversion value when the current is 500 A will be 0 V for Vo, and when the current is −500 A, it gives 3.3V for Vo. This Vo value then enters the microcontroller ADC.

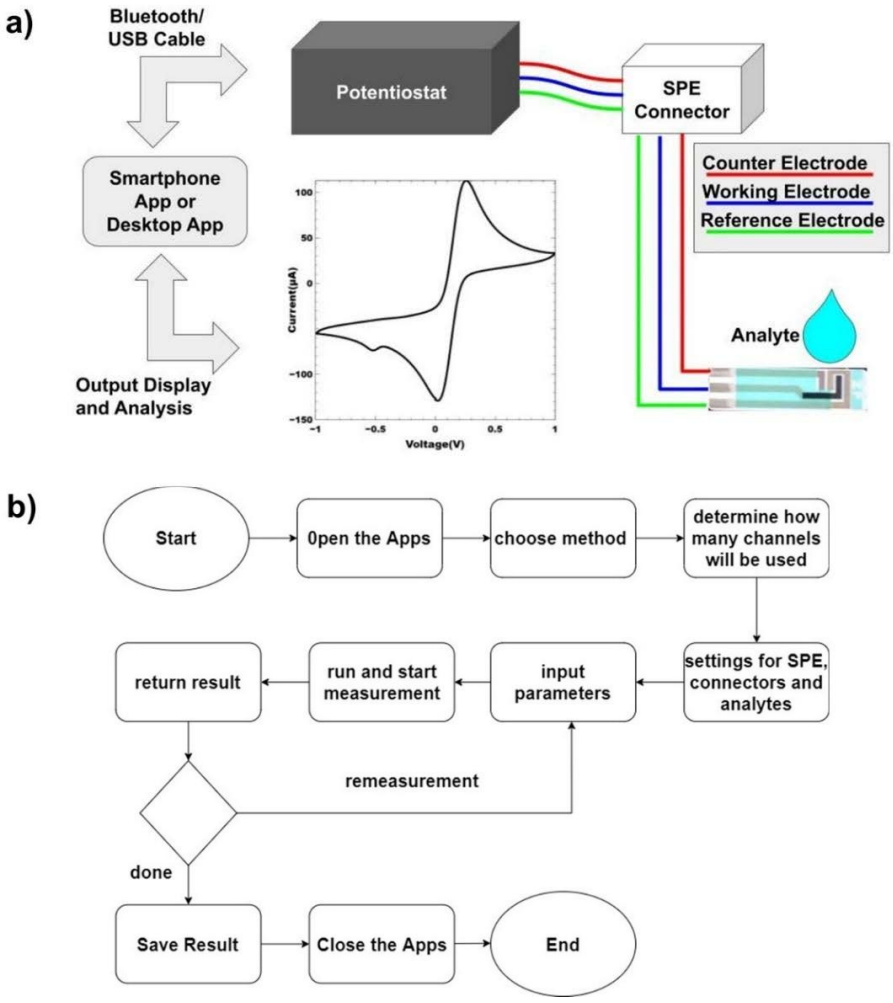

FIGURE 1. a) Schematic of ESPotensio system. b) Flowchart of ESPotensio applications.

Similar to the summing amplifier circuit, there is a voltage shifter block. The addition of a capacitor in this circuit serves to provide a low-pass filter.

In the last circuit block, the buffer block is again used to amplify the output signal, so that the values read in the ADC can be ensured to be more accurate. The signal will also enter the voltage regulator circuit, which ensures this voltage output does not exceed the voltage limit of the ESP32, which is 3.3 V. The voltage regulator circuit was implemented using a reverse-biased 3.3 V Zener diode component. Using this configuration, in the case where the rated output voltage of the circuit exceeds 3.3 V, the current will flow to the Zener diode, which is connected in series with a LED indicator. If it lights up, there is a current flowing and indicates that a voltage exceeds the required limit so that the user can immediately cut off or end the measurement forcibly to prevent damage.

The designed potentiostat uses several component modules that are integrated with analog circuits. There is a microcontroller that functions as the main control for the designed potentiostat. In addition to acquire analog data and convert it into digital form, the microcontroller can also function as a system processor. This module is also tasked with transferring data obtained from measurements from potentiostats to external devices and receiving commands from external devices to potentiostats using BLE and cables via serial communication. The DAC module used in this study is MCP4725. It has a resolution specification of 12 bits. Using this module, the DAC that will enter the analog system will have a higher resolution so that the data obtained will be more precise than the DAC provided by ESP32, which is only 8 bits. The negative voltage serves to supply a negative voltage of −5 V to the IC components. The module will accept the 5 V input supplied from the step-up module, then enter the negative voltage section of the IC. The negative voltage released from this module will experience a slight drop of about 0.1 V to 0.2 V, so the supply voltage from the step-up was set to increase slightly to 5.2V. The negative voltage converter module used in this study is LM2662, while the step-up module used is MT3608.

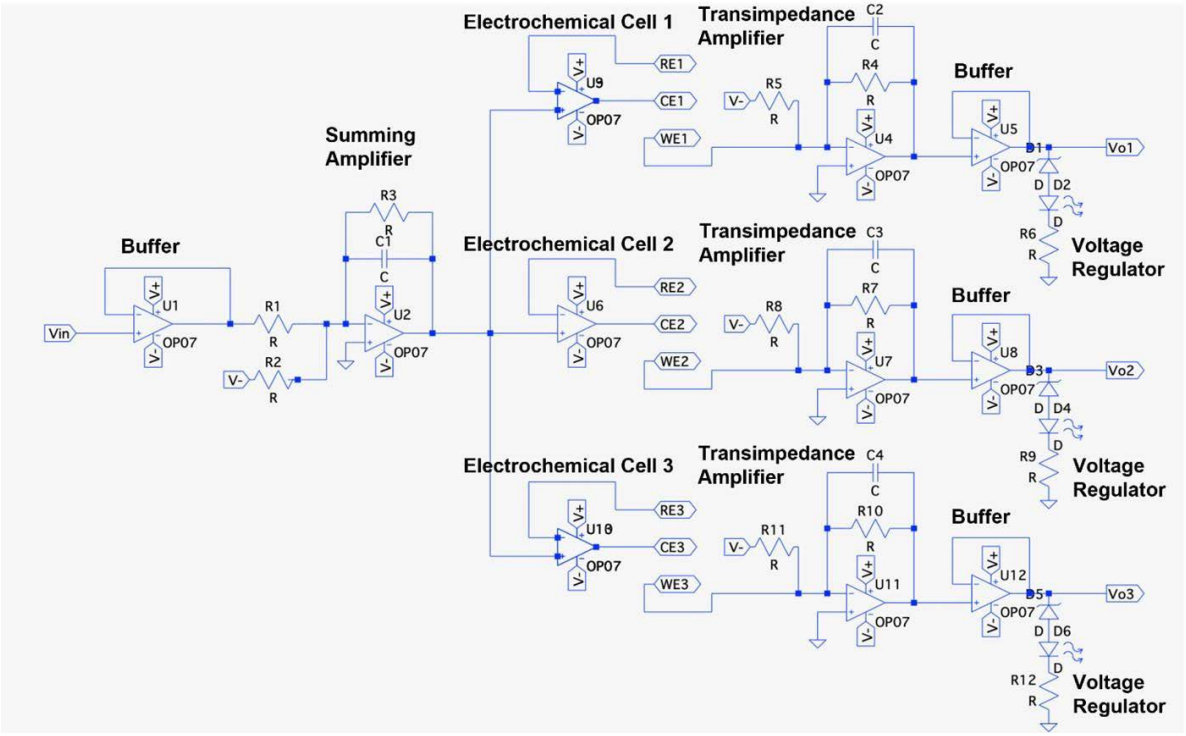

FIGURE 2. Schematic design of the analog front-end circuit of ESPotensio.

The system will receive two different kinds of energy supply in both modes. When taking measurements using a desktop GUI, the energy supply will go together via a USB cable which functions as a data communication medium. The supplied voltage when using a USB cable is 5 V. Meanwhile when using the Android GUI, the energy supply will use a 6 V battery composed of four batteries with 1.5 V in series. This supply goes through the Vin pin of the ESP32. The difference between these two supply voltages makes the system choose two different conditions if these two voltages are directly entered into the negative voltage converter module and the Ic component. The supply voltage is taken from ESP on the 3.3V pin and then increased using a step-up module to uniform the voltage that supplies the IC components even though the energy sources have different voltages.

D. MEASUREMENT METHODS

1) CYCLIC VOLTAMMETRY (CV)

Basically, CV is a method used to determine the relationship between redox peaks and voltammetry. The voltammetric peaks are caused by the specific redox reaction between molecules present in the biological sample and the electrolyte solution, and the current amplitude at each peak strongly correlates with the concentration of that molecules [11]. Therefore, performing a CV test is a must for a potentiostat to analyze the redox species by observing the oxidation and reduction potentials.

The acquisition program for CV begins by inputting the measurement parameters data directly by the user. These include the minimum and maximum sweep voltage limits, the scan rate, and the number of measurement cycles. Afterward, the program will convert the value of this voltage limit into a bit rate of 0 to 4095. The program will later use this conversion to run a loop function for the sweep voltage generation process and ADC readings on each value. At each iteration of the loop function, the program generates a voltage based on its bit rate value at the DAC pin. The voltage at this DAC pin will be as the input to the analog circuit and used as a sweep voltage. Additionally, the program will also record the current measurement values generated through the voltage signal that goes to the ADC pin in each loop. The scan rate parameter determines how fast the voltage sweep is applied to the sample. The scan rate was implemented using a delay.

2) LINEAR SWEEP VOLTAMMETRY (LSV)

The process that occurs in LSV is similar to CV. The difference between these two methods is only in the voltage sweep. In LSV, the sweep voltage only runs linearly in one area without reverse voltage. The parameters used for LSV are also the same as the CV method, i.e. the minimum and maximum sweep voltage, the scan rate, and the number of measurement cycles. An example study on LSV has been used to determine VOR levels by implementing simple carbon nanotube-modified stencil-printed carbon electrodes (CNTs-SP) in pharmaceutical formulations and biological

fluids [12]. By implementing LSV, the efficiency and effectiveness of the electrodeposition process can be increased by evaluating the accurate and precise statistics of the measurement result.

3) DIFFERENTIAL PULSE VOLTAMMETRY (DPV)

If the CV and LSV methods use a sweep voltage to trigger the electrochemical reaction that wants to be observed, then the DPV, SWV, and NPV methods rely on pulses in a given voltage sweep. Therefore, besides the minimum/maximum sweep voltage limit parameters and scan rate, DPV has other parameters: step voltage, pulse voltage, pulse width, and sampling width. In real-life cases, DPV has been used to assist in simultaneously determining seven emerging multiclass contaminants without requiring complex chemometric treatments for quantitative purposes [13] and the rapid detection of the pathogen. By slightly modifying the existing DPV method, it can provide statistically equivalent results to those obtained using the comparative univariate method, which is simpler and faster when compared to traditional calibration.

The step voltage is the value of the increase in the voltage value, which will be the initial basis before the pulse voltage value. DPV has the form of a sweep signal that is linear up but has a rung that is determined by the value of the step voltage and the pulse voltage. The pulse voltage is a drastic increase in the value of the step voltage. The pulse width is the length of time the pulse voltage is given, while the sampling width is the time used to take ADC readings as a sampling measurement. The ADC reading method used is also different from the CV and LSV methods, wherein the pulse voltammetry method, the current value is the result of the difference between the current value for pulse voltage conditions and the current value for step voltage conditions in each loop.

4) SQUARE WAVE VOLTAMMETRY (SWV)

SWV has a similar working principle as DPV. The difference is that the SWV cycle has a negative and positive pulse peak. The current value is read no longer at the step voltage value but at the step voltage value, which has been reduced by the pulse voltage (becomes the negative pulse value), or at the step voltage, which has been added to the pulse voltage (becomes the positive pulse voltage value). A study carried out by SWV could provide observation of the individual curves of the acid and base components [16]. For example, to estimate the pKa of the analyte, which is not possible with conventional pKa estimation methods. Furthermore, SWV was also used to observe the oxidation of aspirin in aqueous solutions at different pH levels in PGE. pKa analysis based on molecular acid and base species curves from voltammetric circuits is an advantage over traditional methods.

5) NORMAL PULSE VOLTAMMETRY (NPV)

From the two pulse voltammetry methods before, NPV has many differences. The voltage sweep pattern in the NPV is no longer linear like DPV and SWV. The NPV sweep voltage pattern has a base voltage value and a pulse voltage, where this pulse voltage will increase each loop by the initial pulse voltage, so the loop will occur until the pulse voltage is close to or equal to the maximum voltage. The sampling voltage and current have the same principle as SWV and DPV. The parameter that distinguishes NPV from SWF and DPV is that in NPV, there is a Vbase parameter and no Vstep parameter. Vbase is the lower voltage value which is the basis for the voltage value before the pulse voltage occurs. This base voltage will be constant until the loop is complete.

Not only used in medical-related research but NPV can also be used to detect leuco-indigo, which plays a role in the dyeing process of Aizome clothes, Japanese indigo-dyeing [15]. Thus, the steady-state concentration profile can be discussed from the kinetics of leuco-indigo microbial generation and their consumption by autoxidation.

6) CHRONOAMPEROMETRY (CA)

CA is quite different from the previous methods, where this method is in a group of amperometry, not voltammetry so that the focus of the readings that will be observed is the current value against time. The number of electrochemical measurement methods can also support data verification in a study. As in another study, a CA sensor protocol was developed for the sensitive and selective measurement of GLY at gold electrodes and then observed the electrochemical behavior of GLY and its aminomethylphosphonic acid (AMPA) metabolites using CV with precious metal electrodes in acidic, neutral, and basic media [16]. So, in this example, CA complements CV to support the results of this study.

TABLE 3. Parameters values used for each electrochemical measurement methods.

Measurement Methods	Parameters Value
CV	V sweep min: -1 V V sweep max:1 V Scan rate: 10 mV/s
DPV	V sweep min: -1 V V sweep max:1 V Scan rate:10 mV/s V amplitude: 0.1 V V increment: 0.005 V Pulse width:100 ms Sampling width: 10 ms
SWV	V sweep min: -0.8 V V sweep max:0.8 V Scan rate:10 mV/s V amplitude/pulse: 0.025 V V increment/step: 0.001 V Pulse width:100 ms Sampling width: 10 ms
NPV	V sweep min: -1 V V sweep max: 1 V Scan rate: 0.01 V/s V base: 0.025 V V increment: 0.01 V Pulse width: 100 ms Sampling width: 10 ms
CA	V dc: 0.05 V Time interval: 0.05 s Running time: 2 s

The working principle of CA is to provide a stable voltage at a certain value, take readings for a certain time, and take samples at certain intervals. The parameters contained in this method are different from the previous methods. CA has parameters such as voltage, running time, and interval time. The voltage parameter is the value of the constant voltage that will be operated into the electrode, while the running time shows the length of the reaction to be carried out. Running time has a very fast value in seconds. The time interval is the sampling time used to read the current value in the ADC. This time interval has a shorter time than the running time in milliseconds. In detail, the parameter values of each measurement method used for testing the performance of the potentiostats are provided in Table 3.

E. COMMUNICATION SYSTEMS

From Fig. 3, it is shown that ESPotensio has two communication systems. Bluetooth communication media was chosen to connect the potentiostat with the application installed on the android smartphone. This media selection is intended to increase the flexibility of using a smartphone with limited battery power and ports when connecting using a cable. The smartphone will detect the presence of existing Bluetooth and the user will connect the Bluetooth smartphone to the potentiostat. The data to be exchanged is serial data. The potentiostat will receive the parameters entered through the application and then the measurement process will be carried out on the potentiostat. Current reading data will be sent in each loop. Finally, the data processing into a CSV file is carried out on the application.

Communication media using a cable is intended for the GUI installed on the Desktop. This use is adapted to the ability of desktop devices, which generally have many ports for USB connectivity, and allows desktop devices to get power supply directly from the mains, so there is no worry about battery power limitations. In the operation of cable communication, it has the same principle as using Bluetooth. The user will enter the desired parameters through the application. The data will be sent via cable and will be processed by the potentiostat. Data will also be sent on each loop by serial communication. The advantage of operating using a cable is a stable data transmission due to the absence of latency and interference by wireless communication.

III. RESULTS AND DISCUSSIONS

A. IMPLEMENTATION OF HARDWARE

The analog circuit schematic design that was previously designed in LTSpice was implemented into a circuit on the PCB. To design the PCB, we use EasyEda Online Design Tool software to integrate module components and analog components. The fully implemented system is shown in Fig. 4a. The casing is fabricated using a 3D printer to cover the entire system including the battery. The final assembly of the system including the casing (Fig. 4b) shows that the portable hardware ESPotensio has a dimension of

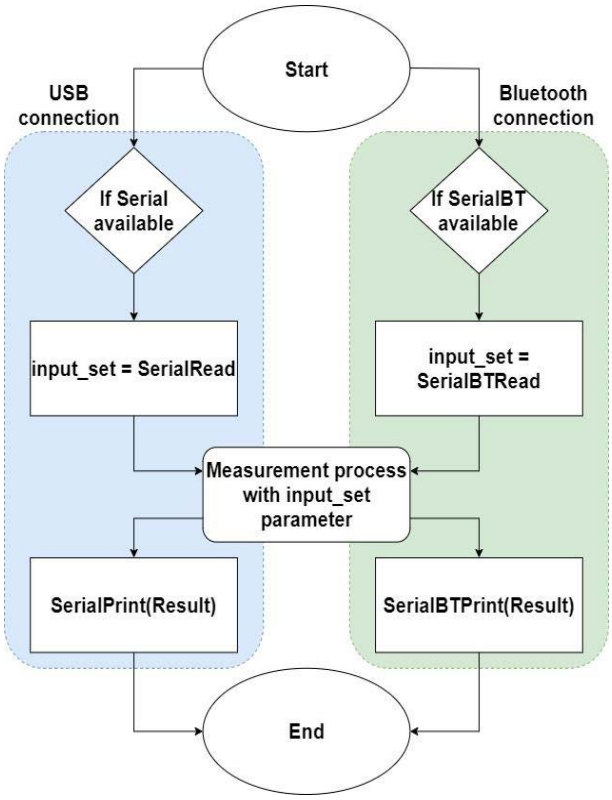

FIGURE 3. ESPotensio communication systems diagram.

10 cm x 9 cm x 5 cm, and as for the Emstat comparison potentiostat, we implemented it into a PCB with a USB to TTL module as shown in Fig. 4c-4d.

Furthermore, the total development cost of the ESPotensio is shown in Table 4. The prices listed are obtained from the Indonesian marketplace, which means the calculated price is a conversion from Rupiah (IDR) to US Dollar (USD). From the calculation, the total cost is only USD 21.4 (without the casing). The casing is optional, and the price strongly depends on the 3D printer vendor, the material selection, and the potentiostat size. The previous version of eSTAT has a higher manufacturing cost because, in this study, we replace the power bank with a battery for power, whereas the cost of installing a power bank in the previous study had reached 25% of the total cost [20]. In addition, in preparing the position for the casing, we manage for the potentiostat to be compact, so that it will reduce the dimensions in the manufacture of the casing.

B. IMPLEMENTATION OF SOFTWARE

In Fig. 5a, we can see the User Interface (UI) of a computer application for ESPotensio. This application is based on the Python programming language utilizing the Tkinter library. In the UI used to operate the ESPotensio using a computer, the user needs to enter several parameters first, namely the name of the file that will be used to save the measurement data in the form of a .CSV file, the number of channels that will

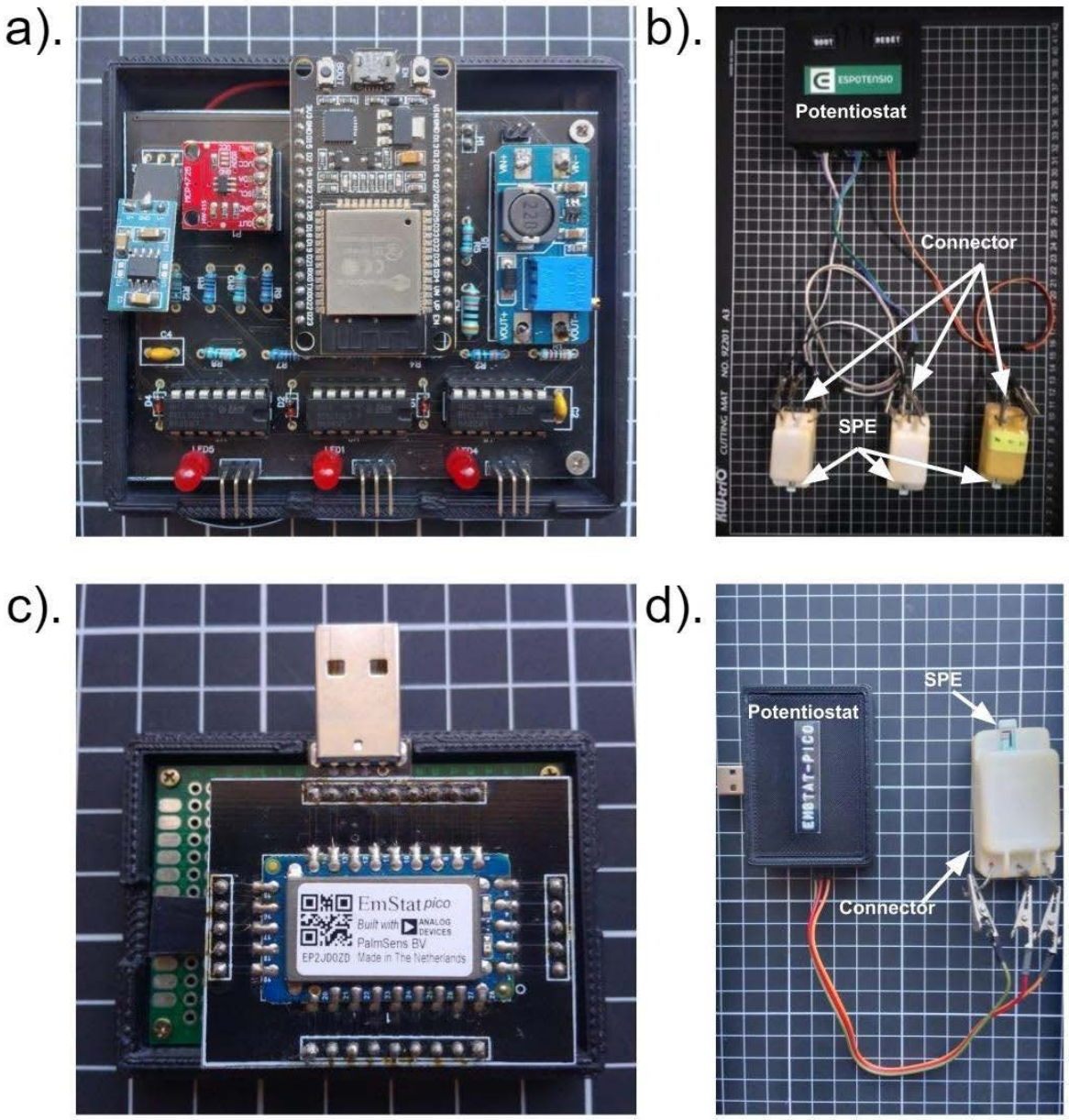

FIGURE 4. Hardware implementation of a) ESPotensio and c) Emstat Pico on the PCB as well as the full hardware implementation of b) ESPotensio and d) Emstat Pico along with the casing and the SPE connectors.

be used in the measurement, then lastly select which method will be used for the measurement. When the measurement method has been selected, the parameter fields related to the parameter settings of the measurement will be opened and the user can enter the desired parameters. After entering the parameters, the user needs to press the RUN button and follow the instructions that appear to wait for the measurement process to complete. The measurement result graph will automatically appear after the measurement is complete.

In Fig. 5b-5d, there are several pages created on the Android application to operate ESPotensio. The application was created using the Java programming language on the Android Studio platform. From the application, the user opens the ESPotensio application, and a Splash Screen appears for 3 seconds, then it will go to the Home Page (Fig. 5b). On this page, several menus are given for electrochemical measurement methods that ESPotensio can carry out. After clicking the menu, the control page for the CV shown in Fig. 5c will appear when the user clicks the CV button. This control view has the same templates for other methods adjusted by setting the appropriate parameters for each method. After entering the appropriate parameters, the user presses the submit button to start the measurement process. Real-time measurement results will appear in the

TABLE 4. Detailed development cost of ESPotensio.

No	Tools and Materials	Quantity	Price per piece (USD)	Total (USD)
1	Electronic Components	1 set	4.18	4.18
2	Microcontroller ESP32	1	5.58	5.58
3	IC LM324	3	0.14	0.42
4	Module LM 2662	1	1.74	1.74
5	Module MCP 4725	1	1.04	1.04
6	Module MT3608	1	0.49	0.49
7	Battery AA 1.5V	4	0.42	1.68
8	PCB Print	1	6.27	6.27
9	3D Printed Casing (optional)	1	17.18	17.18
Total (with casing)				38.58
Total (without casing)				21.4

Measurement Monitor section. By clicking on export to CSV, the measured file will be saved in CSV format and the PLOT button will move the app to the PLOT Page, as shown in Fig. 5d.

C. MULTI-CHANNEL TEST

This test is intended to see the ability of ESPotensio to perform measurements in parallel using its three channels. In this test, observations were made on the CV plot using several resistor values: 2kΩ, 4kΩ, 6kΩ, 8kΩ, and 10kΩ, which the values were determined using a variable resistor. The sweep voltage is set from −1 to 1 V with a scan rate of 50 mV s-1. Based on Fig. 6a-6c, it can be understood that ESPotensio can produce voltammogram plots with a wide range of current measurements according to the ideal range value. The graph shows that the potentiostat potential has produced a linear current plot on the test of the three channels. The three channels have also produced values that have the same characteristics.

The next test is using $K_3[Fe(CN)_6]$ electrolyte solutions at various concentrations: 10 mM, 20 mM, and 30 mM. The electrolytes were diluted in 10 mM of PBS with a pH of 7.4. Two consecutive voltammograms were performed during this validation at potentials between −1 to 1 V (vs. Ag/AgCl). This test shows that the three channels have relatively the same values, as shown in Fig. 6d-6f. The three channels produce values that are almost close to each other.

The data acquisition method used for this multichannel was made semi-parallel. Where in the data acquisition point of view, the microcontroller performs the data retrieval process sequentially alternately for each ADC pin that will represent the current reading. This switch is done very quickly with less than 10 ms. So that by the naked eye, the measurements are carried out as if they were carried out simultaneously.

D. ELECTROCHEMICAL MEASUREMENTS AND PERFORMANCE COMPARISON

The electrochemical measurements using an aqueous solution of $Fe(CN)^{3-/4-}$ ion were used to validate the ability of potentiostats in measuring electrochemical methods.

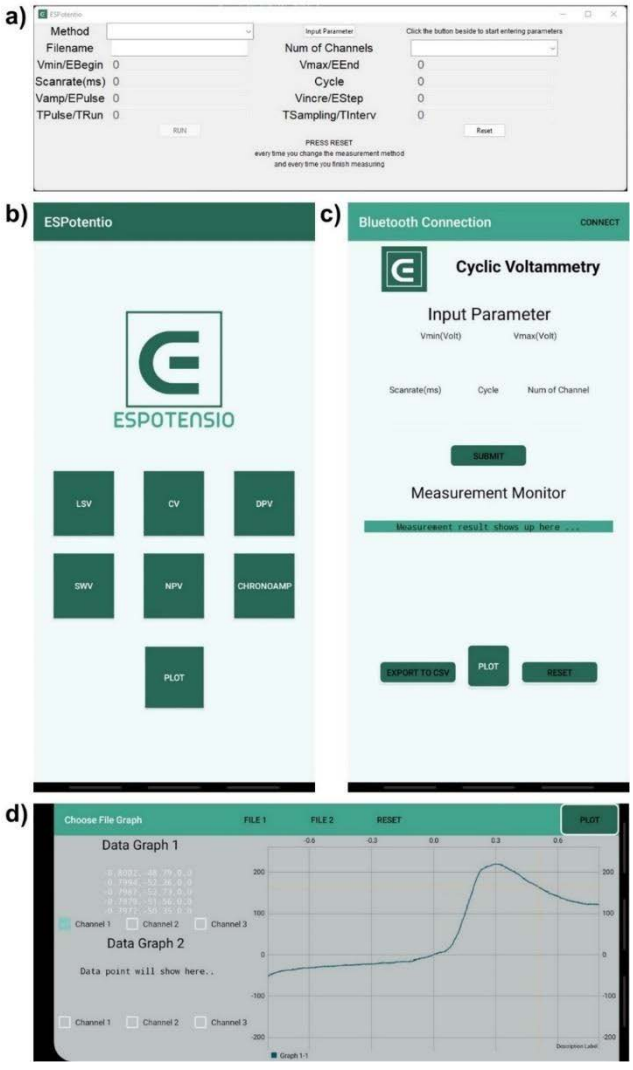

FIGURE 5. ESPotensio GUI. a) Phyton-based UI for communication via wired PC. Mobile and wireless communication of ESPotensio via Android App, including the b) Home Page, c) CV measurement Control Page, and (d) Plot Page.

$Fe(CN)^{3-/4-}$ ion-based electrolyte was used because they have a strong electrochemical reaction, so that it can

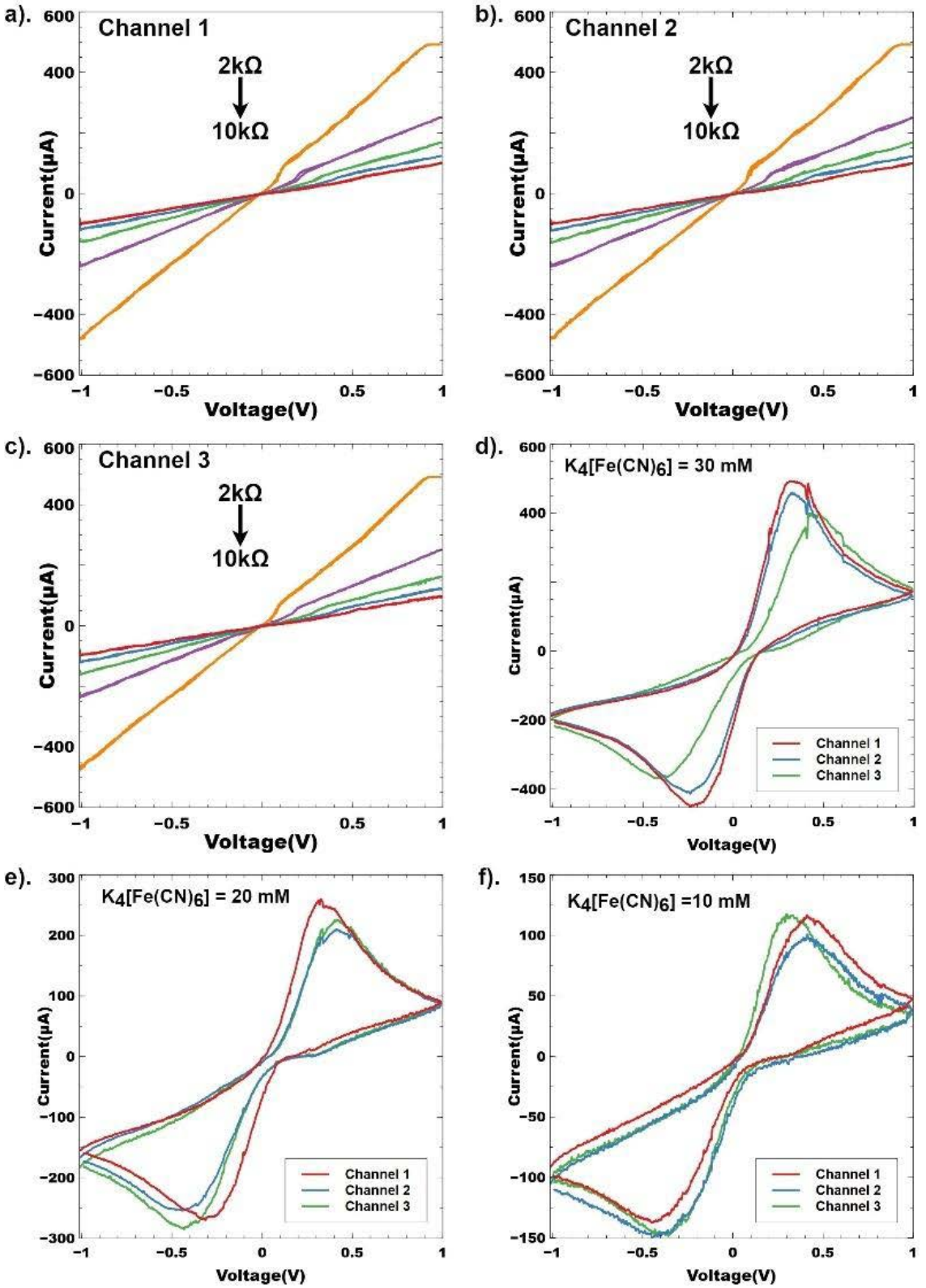

FIGURE 6. Multi-channel CV measurement test using resistors on the corresponding a) Channel 1, b) Channel 2, and c) Channel 3 as well as using d) 10 mM, e) 20 mM, and f) 30mM of K_3 $[Fe(CN)_6]$ electrolyte solution.

demonstrate the concept of reversibility in redox reactions [26], [27]. In this study, the same solution will be used to test all methods offered by ESPotensio and will be compared with commercial potentiostats, specifically Emstat Pico.

TABLE 5. Performance comparison of CV measurement test results.

Cycle	1	2	3	4	5	Average	Precision (±)
Emstat Pico potentiostat							
I_{pa} (μA)	112.76	109.78	111.91	112.76	113.16	112.07	0.984
I_{pc} (μA)	−126.81	−124.82	−124.59	−124.76	−126.44	−125.48	0.912
E_{pa} (V)	0.259	0.251	0.256	0.256	0.256	0.255	0.0022
E_{pc} (V)	−0.145	−0.009	−0.004	0	0	−0.031	0.045
ESPotensio							
I_{pa} (μA)	123	125.71	128.28	129.84	130.24	127.41	2.448
I_{pc} (μA)	−123.52	−125.6	−126.5	−127.28	−127.36	−126.05	1.194
E_{pa} (V)	0.244	0.256	0.261	0.251	0.256	0.253	0.005
E_{pc} (V)	−0.030	−0.030	0	0.003	0.003	−0.054	0.0432
ESPotensio accuracy relative to Emstat Pico potentiostat							
I_{pa} (%)	90.92	85.49	85.37	84.85	84.9	86.3	1.842
I_{pc} (%)	97.4	99.37	98.46	97.98	99.27	98.5	0.66

The performance of the ESPotensio was validated by comparing the anodic (Ipa) and cathodic (Ipc) peak current values with other commercial potentiostats. The comparison product used in this study is Emstat Pico, shown in Fig. 8a.

CV test results can be seen in Table 5. Based on the results, the average accuracy values relative to Emstat Pico in Ipa and Ipc measurements are 86.30% and 98.5%, respectively. Tests carried out with 5 cycles aim to check the precision value that the potentiostat obtained. The instrument's precision values of Ipa and Ipc are ± 2.448 and ±1.194, respectively, with an average relative precision of ±1.82 with Emstat pico.

Furthermore, an experiment to verify the threshold number of cycles for cyclic voltammetry of the ESPotensio has been conducted by applying several cycles of CV for about an hour towards $K_3(FeCN)_6$ analyte sample. The stability test measurement of multiple CV cycles was conducted using two different electrodes, i.e. the screen-printed carbon electrodes from DropSens and from Zimmer-Peacock. This is also to verify that ESPotensio is compatible for different electrodes design. Additionally, the same CV cycles measurement was also conducted using EmStatPico to see how the performance of ESPotensio compared to the commercial potentiostat. As can be seen in Fig. 7, the current density peak value of the CV response is quite stable for 90 cycles with no major drop or rise of the current density peak recorded. However, the 90 cycles number is not exactly the threshold number of cycles as more cycles of CV can actually be applied by the potentiostat. We did not apply more CV cycles as it would be out of the scope of our study, which is not aiming for continuous usage of the potentiostat.

For the LSV test, the results can be seen in Fig. 8b, carried out by providing variations in $K_3[Fe(CN)_6]$ solution concentrations. It can be seen that LSV does not have a reverse voltage which makes the measurement results only have a peak on the graph, where the peak is the reading current plotted against the sweep voltage, which increases linearly

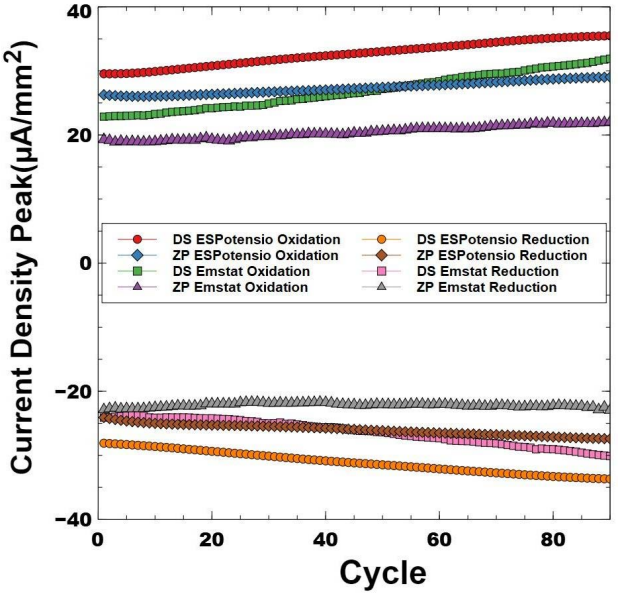

FIGURE 7. The current density peak value of the oxidation and reduction of K_3 $[Fe(CN)_6]$ 20 mM for 90 cycles of CV measurement measured using DropSens and Zimmer Peacock SPEs. The measurement results were compared between ESPotensio and Emstat potentiostat.

from the lower voltage to the upper voltage without any back voltage that can cause a reverse current to appear as in the CV. The summary of the test can be seen in Table 6. The average relative accuracy value for Emstat Pico in Imax is 96.77%, with the relative accuracy of peak current values for measurements with concentrations of $K_3[Fe(CN)_6]$ 10 mM, 20 mM and 30 mM were 99.62%, 98.93%, and 91.78%, respectively.

The results of the DPV test can be seen in Fig. 8c and Table 7. Based on the table, the average relative accuracy value to Emstat Pico in Imax measurements is 98.09%, with

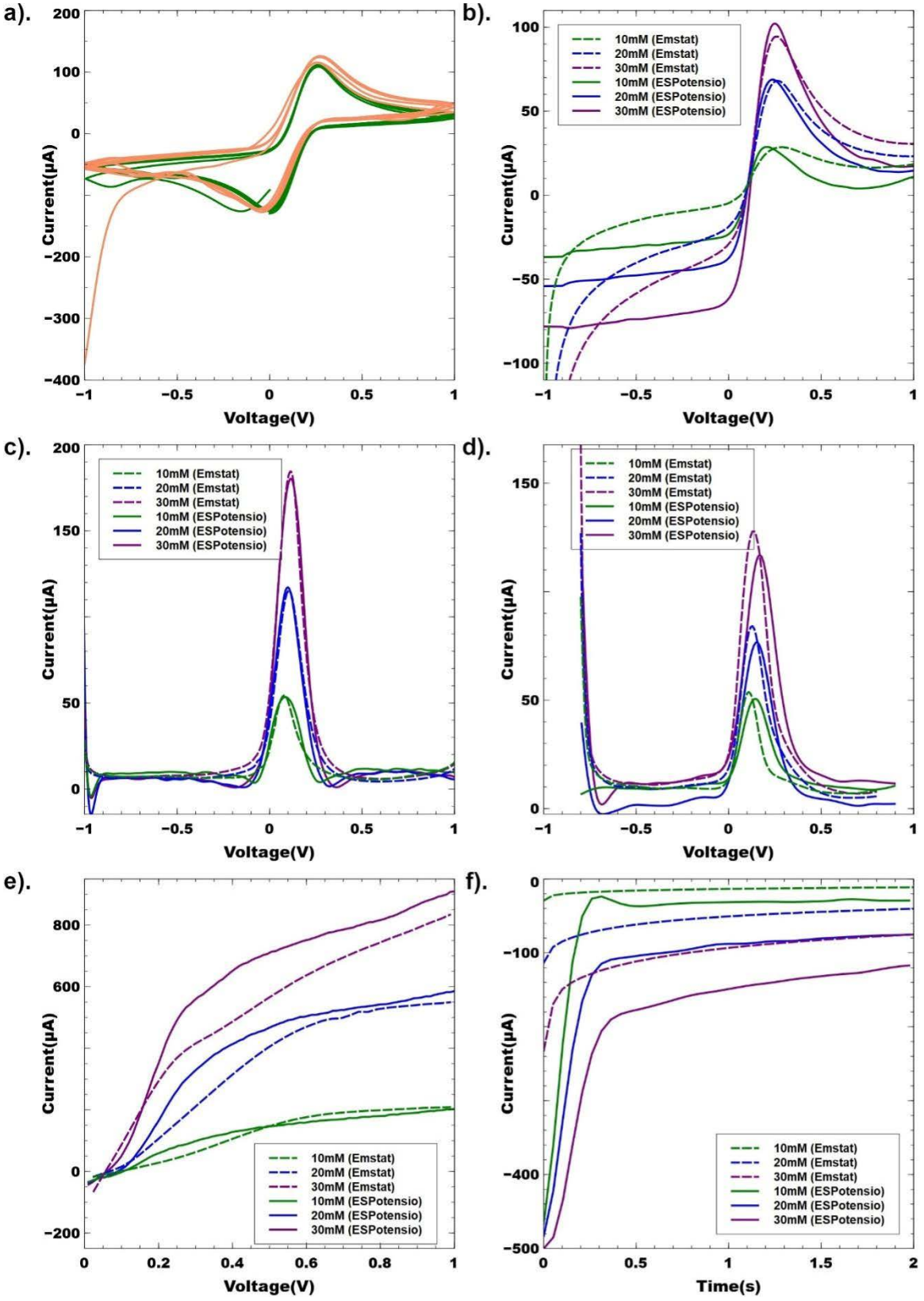

FIGURE 8. a) Comparison of five cycles CV measurement test between Emstat Pico and ESPotensio in 30 mM K_3 $[Fe(CN)_6]$. Comparison of (b) LSV, (c) DPV, (d) SWV, (e) NPV, and (f) CA measurement test results between Emstat Pico and ESPotensio in 10 mM, 20 mM, and 30 mM K_3 $[Fe(CN)_6]$.

TABLE 6. Performance comparison of LSV measurement test results.

Concentration (mM)	10	20	30
Emstat Pico potentiostat			
I_{pa} (μA)	112.76	109.78	111.91
I_{pc} (μA)	−126.81	−124.82	−124.59
ESPotensio			
I_{pa} (μA)	123	125.71	128.28
I_{pc} (μA)	−123.52	−125.6	−126.5
ESPotensio accuracy relative to Emstat Pico potentiostat			
I_{pc} (%)	97.4	99.37	98.46

TABLE 7. Performance comparison of DPV measurement test results.

Concentration (mM)	10	20	30
Emstat Pico potentiostat			
I_{pa} (μA)	54.36	115.20	184.63
I_{pc} (μA)	0.078	0.102	0.112
ESPotensio			
I_{pa} (μA)	53.44	117.15	180.3
I_{pc} (μA)	0.085	0.096	0.113
ESPotensio accuracy relative to Emstat Pico potentiostat			
I_{pc} (%)	98.31	98.31	97.65

TABLE 8. Performance comparison of SWV measurement test results.

Concentration (mM)	10	20	30
Emstat Pico potentiostat			
I_{pa} (μA)	53.85	84.19	127.87
I_{pc} (μA)	0.109	0.128	0.138
ESPotensio			
I_{pa} (μA)	50.64	76.55	117
I_{pc} (μA)	0.147	0.147	0.168
ESPotensio accuracy relative to Emstat Pico potentiostat			
I_{pc} (%)	94.04	90.93	91.50

details of the relative accuracy of peak current values for measurements with concentrations of $K_3[Fe(CN)_6]$ 10 mM, 20 mM, and 30 mM were 98.31%, 98.31%, and 97.65%, respectively. For SWV measurement results can be seen in Fig. 8d and Table 8. Based on the table, the average relative accuracy value to Emstat Pico in Imax measurements is 92.16%, with details of the relative accuracy of peak current values for measurements with concentrations $K_3[Fe(CN)_6]$] 10 mM, 20 mM, and 30 mM were 94.04%, 90.93%, and 91.50%, respectively. NPV and CA show results that resembled the Emstat Pico (Fig. 8e-8f).

In the NPV test, the resulting measurement graph looks almost consistent, showing that the average relative deviation from ESPotensio to Emstat is ± 3.02, as shown in Table 9. Meanwhile, in CA, there is a difference between the ESPotensio measurement graph and the Emstat measurement, even though the graph patterns appear parallel and show the same characteristics; the average relative deviation obtained from ESPotensio to Emstat is ± 34.76, as shown in Table 10.

Noted that for these electrochemical measurements and performance comparison tests, we did not add interfering analytes to the electrolyte solution since to obtain a selective electrochemical measurement, the SPE is needed to be modified chemically (not the potentiostat), which is beyond the scope of our research work.

TABLE 9. Performance comparison of NPV measurement test results.

Concentration (mM)	Std. deviation
10	1.02
20	3.16
30	4.88
Average std. deviation	3.02

TABLE 10. Performance comparison of CA measurement test results.

Concentration (mM)	Std. deviation
10	30.98
20	38.57
30	34.3
Average std. deviation	34.76

IV. CONCLUSION

A low-cost and portable potentiostat has been designed with the ability to perform various electrochemical measurements, including CV, LSV, DPV, SWV, NPV, and CA measurements. To check the potential of the potentiometer, measurements were made by measuring the CV resistor. The performance of the ESPotensio was then compared with a commercial potentiostat, namely Emstat pico to measure the $K_3[Fe(CN)_6]$ solution with relative accuracy value for CV, LSV, DPV, and SWV of more than 90%. Meanwhile, for the NPV, the graph generated from the measurement results looks almost closely, indicating the similarity of the measurement results between ESPotensio and Emstat as an indication of high accuracy values. While in the CA, the graph pattern was appropriate, indicating the same measurement characteristics as the Emstat Pico potentiostat with its module only integrated with the USB module.

We can also see that, in general, potentiostats have one measurement channel, while in this study, we show that three measurement channels can be run semi-parallelly. Moreover, compared to other multichannel potentiostats, ESPotensio has a much lower manufacturing cost despite having the same resolution. Compared to other studies based on ESP32, ESPotensio has several improved specifications compared to the previous version with a much wider and more readable current range with a difference of ±200 μA and a cheaper production cost of around 21 USD, where these costs include the lowest among other studies on low-cost potentiostats. In addition, there is a communication mode with two options, namely Bluetooth for GUI using a smartphone and USB for GUI using a computer application. With this integrated function to Android applications and computers, ESPotensio has superiority for its portability, simplicity, and a wider range of user-friendliness.

REFERENCES

[1] D. Liu, J. Wang, L. Wu, Y. Huang, Y. Zhang, M. Zhu, Y. Wang, Z. Zhu, and C. Yang, "Trends in miniaturized biosensors for point-of-care testing," *TrAC Trends Anal. Chem.*, vol. 122, Jan. 2020, Art. no. 115701, doi: 10.1016/j.trac.2019.115701.

[2] D. Sarpong, G. Ofosu, D. Botchie, and F. Clear, "Do-it-yourself (DiY) science: The proliferation, relevance and concerns," *Technol. Forecasting Social Change*, vol. 158, Sep. 2020, Art. no. 120127, doi: 10.1016/j.techfore.2020.120127.

[3] C.-Y. Huang, H.-T. Huang, and R.-T. Yuan, "Design of a portable mini potentiostat for electrochemical biosensors," in *Proc. IEEE 2nd Adv. Inf. Technol., Electron. Autom. Control Conf. (IAEAC)*, Mar. 2017, pp. 200–203, doi: 10.1109/IAEAC.2017.8054006.

[4] S. Sarkar and M. Bhattacharya, "SStat: Wi-Fi and Bluetooth integrated multimodal 'do-it-yourself' electrochemical potentiostat," in *Proc. 46th Annu. Conf. IEEE Ind. Electron. Soc. (IECON)*, Oct. 2020, pp. 5249–5254, doi: 10.1109/IECON43393.2020.9254701.

[5] S. Adams, E. H. Doeven, K. Quayle, and A. Kouzani, "MiniStat: Development and evaluation of a mini-potentiostat for electrochemical measurements," *IEEE Access*, vol. 7, pp. 31903–31912, 2019, doi: 10.1109/ACCESS.2019.2902575.

[6] P. Pansodtee, J. Selberg, M. Jia, M. Jafari, H. Dechiraju, T. Thomsen, M. Gomez, M. Rolandi, and M. Teodorescu, "The multi-channel potentiostat: Development and evaluation of a scalable mini-potentiostat array for investigating electrochemical reaction mechanisms," *PLoS ONE*, vol. 16, no. 9, Sep. 2021, Art. no. e0257167, doi: 10.1371/journal.pone.0257167.

[7] S. Bukkawar, N. Sarwade, M. S. Panse, and H. Muthurajan, "Design and development of portable potentiostat for advanced research in electrochemical biosensing," in *Proc. IEEE Int. Conf. Power, Control, Signals Instrum. Eng. (ICPCSI)*, Sep. 2017, pp. 2531–2535, doi: 10.1109/ICPCSI.2017.8392173.

[8] Y. C. Li, E. L. Melenbrink, G. J. Cordonier, C. Boggs, A. Khan, M. K. Isaac, L. K. Nkhonjera, D. Bahati, S. J. Billinge, S. M. Haile, R. A. Kreuter, R. M. Crable, and T. E. Mallouk, "An easily fabricated low-cost potentiostat coupled with user-friendly software for introducing students to electrochemical reactions and electroanalytical techniques," *J. Chem. Educ.*, vol. 95, no. 9, pp. 1658–1661, Sep. 2018, doi: 10.1021/acs.jchemed.8b00340.

[9] M. W. Glasscott, M. D. Verber, J. R. Hall, A. D. Pendergast, C. J. McKinney, and J. E. Dick, "SweepStat: A build-it-yourself, two-electrode potentiostat for macroelectrode and ultramicroelectrode studies," *J. Chem. Educ.*, vol. 97, no. 1, pp. 265–270, Jan. 2020, doi: 10.1021/acs.jchemed.9b00893.

[10] Z. H. Ning, J. Q. Huang, S. X. Guo, and L. H. Wang, "A portable potentiostat for three-electrode electrochemical sensor," *J. Phys., Conf.*, vol. 1550, no. 4, May 2020, Art. no. 042049, doi: 10.1088/1742-6596/1550/4/042049.

[11] H.-W. Wang, C. Bringans, A. J. R. Hickey, J. A. Windsor, P. A. Kilmartin, and A. R. J. Phillips, "Cyclic voltammetry in biological samples: A systematic review of methods and techniques applicable to clinical settings," *Signals*, vol. 2, no. 1, pp. 138–158, Mar. 2021, doi: 10.3390/signals2010012.

[12] M. El Henawee, H. Saleh, A. K. Attia, E. M. Hussien, and A. R. Derar, "Carbon nanotubes bulk modified printed electrochemical sensor for green determination of vortioxetine hydrobromide by linear sweep voltammetry," *Measurement*, vol. 177, Jun. 2021, Art. no. 109239, doi: 10.1016/j.measurement.2021.109239.

[13] D. A. Gonçalves, J. S. Carmo, L. T. S. Zanon, B. S. Marangoni, C. Cena, G. A. Camara, G. L. Donati, and M. A. G. Trindade, "Simultaneous quantification of seven multi-class organic molecules by single-shot dilution differential pulse voltammetric calibration," *Talanta*, vol. 237, Jan. 2022, Art. no. 122975, doi: 10.1016/j.talanta.2021.122975.

[14] Z. Yazan, D. Eskiköy Bayraktepe, and E. Dinç, "Square wave voltammetric pKa determination of aspirin using multi-way data analysis models," *Chem. Papers*, vol. 76, no. 9, pp. 5389–5397, Sep. 2022, doi: 10.1007/s11696-022-02250-9.

[15] M. Kikuchi, K. Sowa, M. Takeuchi, K. Nakagawa, M. Matsunaga, A. Ando, K. Kano, J. Ogawa, and E. Sakuradani, "Quantification of leuco-indigo in indigo-dye-fermenting suspension by normal pulse voltammetry," *J. Biosci. Bioeng.*, vol. 134, no. 1, pp. 84–88, Jul. 2022, doi: 10.1016/j.jbiosc.2022.04.009.

[16] B. Uka, J. Kieninger, G. A. Urban, and A. Weltin, "Electrochemical microsensor for microfluidic glyphosate monitoring in water using MIP-based concentrators," *ACS Sensors*, vol. 6, no. 7, pp. 2738–2746, Jul. 2021, doi: 10.1021/acssensors.1c00884.

[17] P. Irving, R. Cecil, and M. Z. Yates, "MYSTAT: A compact potentiostat/galvanostat for general electrochemistry measurements," *HardwareX*, vol. 9, Apr. 2021, Art. no. e00163, doi: 10.1016/j.ohx.2020.e00163.

[18] K. Krorakai, S. Klangphukhiew, S. Kulchat, and R. Patramanon, "Smartphone-based NFC potentiostat for wireless electrochemical sensing," *Appl. Sci.*, vol. 11, no. 1, p. 392, Jan. 2021, doi: 10.3390/app11010392.

[19] A. V. Cordova-Huaman, V. R. Jauja-Ccana, and A. La Rosa-Toro, "Low-cost smartphone-controlled potentiostat based on Arduino for teaching electrochemistry fundamentals and applications," *Heliyon*, vol. 7, no. 2, Feb. 2021, Art. no. e06259, doi: 10.1016/j.heliyon.2021.e06259.

[20] J. Monge, O. Postolache, A. Trandabat, and S. Macovei, "Multi-node potentiostat device and multiplatform mobile application for on-field measurements," in *Proc. Int. Conf. Expo. Electr. Power Eng. (EPE)*, Oct. 2020, pp. 695–698, doi: 10.1109/EPE50722.2020.9305567.

[21] O. S. Hoilett, J. F. Walker, B. M. Balash, N. J. Jaras, S. Boppana, and J. C. Linnes, "KickStat: A coin-sized potentiostat for high-resolution electrochemical analysis," *Sensors*, vol. 20, no. 8, p. 2407, Apr. 2020, doi: 10.3390/s20082407.

[22] P. Wu, G. Vazquez, N. Mikstas, S. Krishnan, and U. Kim, "Aquasift: A low-cost, hand-held potentiostat for point-of-use electrochemical detection of contaminants in drinking water," in *Proc. IEEE Global Humanitarian Technol. Conf. (GHTC)*, Oct. 2017, pp. 1–4, doi: 10.1109/GHTC.2017.8239306.

[23] V. Bianchi, A. Boni, S. Fortunati, M. Giannetto, M. Careri, and I. de Munari, "A Wi-Fi cloud-based portable potentiostat for electrochemical biosensors," *IEEE Trans. Instrum. Meas.*, vol. 69, no. 6, pp. 3232–3240, Jun. 2020, doi: 10.1109/TIM.2019.2928533.

[24] V. Bianchi, A. Boni, M. Bassoli, M. Giannetto, S. Fortunati, M. Careri, and I. De Munari, "IoT and biosensors: A smart portable potentiostat with advanced cloud-enabled features," *IEEE Access*, vol. 9, pp. 141544–141554, 2021, doi: 10.1109/ACCESS.2021.3120022.

[25] I. Anshori, G. F. Mufiddin, I. F. Ramadhan, E. Ariasena, S. Harimurti, H. Yunkins, and C. Kurniawan, "Design of smartphone-controlled low-cost potentiostat for cyclic voltammetry analysis based on ESP32 microcontroller," *Sens. Bio-Sensing Res.*, vol. 36, Jun. 2022, Art. no. 100490, doi: 10.1016/j.sbsr.2022.100490.

[26] S. Petrovic, "Cyclic voltammetry of hexachloroiridate (IV): An alternative to the electrochemical study of the ferricyanide ion," *Chem. Educator*, vol. 5, no. 5, pp. 231–235, Oct. 2000, doi: 10.1007/s00897000416a.

[27] S. Chandra, W. Tupiti, S. Singh, Z. Naaz, P. K. Kishor, A. Goundar, M. Fakraufon, and S. Prasad, "An undergraduate-level electrochemical investigation of gold nanoparticles-modified physically small carbon electrodes," *World J. Chem. Educ.*, vol. 4, no. 5, pp. 93–100, 2016.

ISA ANSHORI received the B.Eng. degree from the Engineering Physics Department, Bandung Institute of Technology, Indonesia, in 2009, and the M.Eng. degree in materials science and the Ph.D. degree in nanoscience and nanotechnology from the University of Tsukuba, Japan, in 2015 and 2018, respectively. He has been working as an Assistant Professor with the Biomedical Engineering Department, Bandung Institute of Technology, since 2018. His current research interests include bio/chemical sensors, microfluidics, the IoT devices, and lab-on-chip.

IQBAL FAWWAZ RAMADHAN received the bachelor's degree in electrical engineering, with the topic of the final project of making a prototype cryptocurency hardware wallet and the master's degree with a focus on biomedical engineering from the Bandung Institute of Technology, in 2020 and 2022, respectively. His master's thesis is on the manufacture of a potentiostat biosensor reading device. His research interests include the fields of biomedical instrumentation, the IoT, machine learning, and data analysis, and research related to IC architectural design.

EDUARDUS ARIASENA received the B.Sc. degree from the Biomedical Engineering Department, Bandung Institute of Technology, Indonesia, in 2022. His research interests include electrochemical biosensors and nanotechnology-related topic.

RIKSON SIBURIAN received the B.S. and M.S. degrees in chemistry from the University of Sumatera Utara, in 1998 and 2001, respectively, and the Ph.D. degree in pure and applied science from the University of Tsukuba, in 2013. He is currently an Associate Professor with the Chemistry Department, University of Sumatera Utara, and affiliated with the Carbon Research Center, University of Sumatera Utara.

JON AFFI received the bachelor's degree in mechanical engineering from the University of Andalas, Padang, in 1997, the master's (Magister) degree in engineering from the Bandung Institute of Technology, in 2002, and the Doctor of Engineering degree in mechanical and structural system engineering from the Toyohashi University of Technology, in 2012. He is currently an Associate Professor with the Mechanical Engineering Department, Faculty of Engineering, University of Andalas. He started his carrier as a Lecturer, in 1998. His research interest in the past ten years was coating, joining, biomaterial engineering, and graphene.

MURNI HANDAYANI received the B.Sc. degree from the Chemistry Department, Sebelas Maret University, Indonesia, in 2003, and the M.Sc. and Ph.D. degrees from the Chemistry Department, Osaka University, Japan, in 2013 and 2016, respectively, under supervision of Prof. Takuji Ogawa. After her doctoral graduation, in 2017, she was a Specially Assigned Assistant Professor with the Chemistry Department, Osaka University. She was a Visiting Scientist with Nanyang Technological University (NTU), Singapore, and TU Braunschweig, Germany, in 2019. From 2005 to 2021, she was a Researcher with the Research Center for Metallurgy and Materials, Indonesian Institute of Sciences (LIPI). In 2021, the Indonesian Institute of Sciences merged into the National Research and Innovation Agency (BRIN). She is currently a Researcher with the Research Center for Advanced Materials, National Research and Innovation Agency (BRIN). Her current research interests include nanoscience, advanced materials synthesis, molecular architectonics, nanocomposites and nanomaterials, especially nanocarbons (graphene and carbon nanotubes).

HENKE YUNKINS received the B.S.E.E. degree from Purdue University, in 2001.

His projects included developing a directional hearing aid for the Purdue EPICS program, while also completing a fellowship with NSF REU on the topic of Speech Language Recognition. After graduation, he worked at Xilinx, a fabless semiconductor company, as an Application Engineer. He was responsible for FPGA applications materials pertaining to timing, digital clock management and multiplexers, and BRAM and ECC memory controllers, and LocalLink re-transmission. Later, he developed FPGA dynamic power models as a Product Engineer. In 2013, he co-founded Phire Studio, Indonesia. The company focus is creating and developing industrial IoT and intelligent solutions using AI and automated analytics. In 2018, Phire Studios expanded operations into Singapore, and in 2019, launched PhiBase, its entry into the Industry 4.0 space. PhiBase has since been deployed to dozens of customers in several different industries and countries. In 2021, he worked on a BPPT task force, setting up the AI Ethics Principles for Indonesia National AI Strategy. Currently, he works as the Director of Regulation and Ethics for Indonesian AI Society. His research interests include the IoT and the IoT communication solutions, artificial intelligence, analytics, applied technologies in the areas of human well-being, and health care, and conducting research in nano technology, sensor technologies, and optimization algorithms.

TOMOAKI KUJI received the Ph.D. degree from the Graduate School of Comprehensive Human Sciences, University of Tsukuba, in 2022.

He is currently a CEO of Japanese startup company president, Blue Industries Inc., which he started, in 2015. The company focused on research and development of portable device and postal diagnostic service and has an access with consumable manufacturers, medical device manufacturers, and universities to conduct research and development. Most recently, he has been working with investors to develop new mailing inspection technologies.

TATI LATIFAH ERAWATI RAJAB MENGKO received the bachelor's degree in electrical engineering from the Institut Teknologi Bandung, Bandung, Indonesia, in 1977, and the Ph.D. degree from the École Nationale Supérieure d'Électronique et de Radioélectricité de Grenoble (ENSERG), Institut National Polytechnique de Grenoble, France, in 1985, where she studied texture-based image processing. Since 2005, she has been a Professor with the School of Electrical Engineering and Informatics, ITB, where she is currently the Head of the Biomedical Engineering Research Group. Her research interests include biomedical signal and image processing.

SUKSMANDHIRA HARIMURTI received the B.S. degree in engineering physics from the Institut Teknologi Bandung, Indonesia, in 2012, and the M.Eng. degree in electrical engineering from The University of Tokyo, Japan, in 2015. From 2016 to 2018, he was appointed as a Research Fellow at the Microelectronics Center Institut Teknologi Bandung. He was a technical team leader for various research projects both local and international (including with the local IC design house and international chip foundry). Since 2019, he has been a Research Associate and a Teaching Assistant at the Department of Biomedical Engineering Institut Teknologi Bandung. He was the main technical contributor for several basic and industrial research projects in the Department, such as the Non-Invasive Vascular Analyzer (NIVA) and the Portable Hepatitits Virus Sensor System projects. His research interests include wearable and flexible electronics, biosensors, biomedical science and engineering, embedded systems, sensors and systems, and VLSI and RF analog integrated circuits (IC) design for smart card and biomedical applications.